16th World Conference on Earthquake, 16WCEE 2017

Santiago Chile, January 9th to 13th 2017

Paper N° 234

Registration Code: S-Z1463158322

PLASTICITY SPREAD IN COLUMNS REINFORCED WITH HIGH STRENGTH STEEL

D. Sokoli [1], A. Limantono [2], W. M. Ghannoum [3]

[1] *Graduate Student, The University of Texas at Austin, drit@utexas.edu*
[2] *Project Engineer, Hollingsworth Pack, albert.l@holl-pack.com*
[3] *Associate Professor, The University of Texas at San Antonio, wassim.ghannoum@utsa.edu*

Abstract

The demand for higher strength reinforcing steel in concrete construction is rapidly increasing in the United States and worldwide. Economic, environmental, and contractibility incentives are fueling the demand, particularly in highly congested seismic designs. Nevertheless, current code limits on the strength of reinforcing steel in the U.S, combined with a lack of understanding of the effects of higher strength steel on the performance of concrete members, are hindering progress in structural designs. Steel grades higher than Grade 80 (80 ksi specified yield strength [540 MPa]) and having relatively high ductility (>10% fracture strains) are just emerging in the U.S. However, the steel industry is producing the high-strength steels with varying mechanical properties. Test results are presented from an experimental program carried at the University of Texas at Austin aimed at evaluating the effect of the tensile-to-yield (T/Y) strength ratio of high-strength reinforcement on the plasticity spread in concrete columns subjected to seismic demands. Comparisons are made between the performances of columns reinforced with various grade bars including Grade 100 bars (100 ksi specified yield strength [690 MPa]) produced using the leading production techniques in the U.S. and having different T/Y strength ratios. These tests were conducted as part of a research effort aimed at setting the minimum acceptable T/Y ratio in new ASTM specifications for seismic Grades 80 and 100 reinforcement. Column specimens were tested under constant axial load and reverse cyclic lateral loading until significant loss in lateral load carrying capacity. Conclusions are drawn with respect to the effects of higher strength reinforcement on the seismic performance of concrete columns and strain demands on reinforcing bars.

Keywords: reinforced concrete; high strength steel; seismic; shear; columns

1. Introduction

High strength reinforcing steel has the potential to provide the structural engineering society with more effective design solutions for reinforced concrete structures. Besides offering one more variable which could be altered to fit specific designs, the use of higher grades of reinforcing bars has the potential to reduce bar congestion in concrete construction. Economic and environmental considerations are also major contributors to the demand for higher strength reinforcement.

High strength reinforcing bars (HSRBs) are defined here as reinforcing bars having a yield strength of 80 ksi (540 MPa) or more. Current building codes limit the strength of reinforcing steel to be used in design of concrete members. The ACI 318-14 building code [1] limits the reinforcement strength to 80 ksi (540 MPa) for non-seismic systems except for shear, which has to be designed using a maximum yield strength for transverse reinforcement of 60 ksi (415 MPa). For seismic design, the limit currently remains at 60 ksi (415 MPa). Grade 100 (690 MPa) steel was recently allowed in the ACI building code but only for confinement. Performance concerns coupled with a lack of experimental investigations have maintained such limits to this day. As a primary concern, higher grade reinforcement is associated with lower ductility. High strength steel also yields at a higher strain, which can lead to larger deflections and crack-widths in members. Larger cracks can impair the aggregate interlock mechanism reducing the shear strength of the section.

Previous work has shown that a low value of the tensile-to-yield strength ratio (*T/Y*) can produce higher strain concentrations in bars at cracks [2, 3, 4, 5, 6]. Strain concentrations in the longitudinal reinforcement can cause premature bar fracture, leading to lower member deformation ductility. Aoyama [2] reported tests on beams reinforced with high-strength bars. Two different types of reinforcing bars were used in the study. The R90 bars had a relatively low *T/Y* ratio of 1.1, while the CR75 bars had a higher *T/Y* ratio of 1.33. Failure was reported to occur due to longitudinal bar fracture at an earlier loading stage in the beams with the steel having a low T/Y ratio; at a lateral drift ratio of 5%. The researchers concluded that a lower tensile to yield ratio results in substantially larger bar strains for the same lateral deformation. As part of another investigation, twenty-seven small-scale columns with two different reinforcing steel properties were tested cyclically in single curvature by Macchi et.al. [3]. The first type of steel bars used, named A8, had a yield strength of 87 ksi (600 MPa), a *T/Y* ratio of 1.1, and a uniform elongation of 0.08. Uniform elongation is defined as the bar elongation at peak stress. The second type of steel bars used, named Fe, had a yield strength of 86 ksi (593 MPa), a *T/Y* ratio of 1.4, and a uniform elongation of 0.11. Specimens with varying cross sections and longitudinal and transverse reinforcement layouts were tested under three different loading protocols. Applied axial loads varied from 0 to 16% $A_g f'_c$ (where A_g = gross sectional area; f'_c = concrete compressive strength). In all cases, failure was observed due to longitudinal bar fracture. Specimens reinforced with A8 bars were reported to have failed before completing the target loading protocol. In contrast, concrete columns reinforced with Fe bars had failed after completing the loading protocol in all cases. The authors concluded that the earlier bar fractures in columns reinforced with A8 bars, were mainly attributed to strain concentrations in the longitudinal reinforcement and limited flexural plasticity spread. Strain hardening, or the *T/Y* ratio, was observed to have a larger effect on the overall behavior of the members than fracture elongation values. The authors recommend a minimum *T/Y* ratio of 1.3 for seismic applications, which is close to the minimum specified *T/Y* ratio of 1.25 in the ASTM A706 standard [7] for bars intended for seismic applications.

This paper presents experimental results from a completed study [5, 6] and an ongoing one that investigated the use of high strength reinforcement in concrete columns. The studies used recently developed high-strength bars in the U.S. Particularly, the implications of longitudinal bar ductility and *T/Y* ratios on the plasticity spread and deformation capacity of concrete columns are presented. The impacts of these bar properties on bar strain concentrations and associated cyclic fatigue demands are also discussed.

2. Experimental Program

This paper presents results from experimental tests on five concrete columns reinforced with bars having different strengths and mechanical properties. These tests were carried out in two series. The first series was reported in previous work done by the authors [6, 7] and consists of three columns: CS60, CS80, and CS100.

Series 1 tests were designed to assess the performance of high-strength transverse bars under high shear and confinement demands. These specimens had identical dimensions, with primary variables being the grade of reinforcement and associated bar sizes and spacing. Grade 60, 80, and 100 longitudinal and transverse bars were used in columns CS60, CS80, and CS100, respectively. The second series focused on investigating the effects of the *T/Y* ratio of longitudinal bars on strain concentrations and flexural plasticity spread. Specimens in Series 2 were dubbed CL100 and CH100, referring to the low and high *T/Y* ratio of the Grade 100 (690 MPa) reinforcement used respectively in each specimen. The Grade 100 (690 MPa) reinforcement used in both series are a result of a recent push by the U.S. steel manufacturers in producing high-strength reinforcing bars (HSRB) with relatively high ductility. Columns from both series satisfied most of the seismic provisions for Special Moment Frames of ACI 318-14. Columns did not contain any lap splices. Columns framed into two end-blocks in which the longitudinal bars were anchored using standard ACI 318-14 hooks or headed bars. All longitudinal and transverse bars for all specimens were bent to current ACI 318-14 bend radii.

2.1 Specimen Description

The geometry, measured material properties, and reinforcement details for all columns are given in Table 1, Table 2 and Figure 1. All specimens had square cross sections with $b = h = 18$ in. (457 mm) (see Tables 1 and 2 for definition of notations).

Series 1 columns, CS60, CS80, and CS100, had a clear span of 84 in. (2160 mm). The clear cover (*cc*) in these specimens was 1.5 in. (38 mm). The targeted compressive strength was 4.5 ksi, and the measured concrete compressive strengths (f'_c) at the day of testing are given in Table 1. These columns were tested under relatively high axial load (P_o), corresponding to about 29% of the gross section capacity. The three specimens were designed to achieve similar flexural strengths with the same arrangement of 12 longitudinal bars. Smaller bar sizes were used for specimens with higher grades of reinforcement. Relatively high longitudinal steel ratios were used to drive high shear demands in members. The expected plastic moment strengths (M_p), calculated using fiber section analysis with measured materials properties (f_y and f'_c) were between 6,900 kip-in. (800 kN-m) and 7,300 kip-in. (825 kN-m), corresponding to peak shear demands (V_e) of 165 (734 kN) to174 kips (774 kN). The expected peak shear stress ($V_e/bd\sqrt{f'_c}$) was in the order of $10\sqrt{f'_c}$ (in psi units; $0.83\sqrt{f'_c}$ *in MPa units*). The imposed maximum shear stress was selected such that hoop design was governed by shear and not confinement requirements. As flexural yielding was intended in the tests, the shear strength of the column was designed to be larger than V_e/φ (with $\varphi = 0.75$ as per ACI 318-14). Therefore, the steel contribution to shear strength (V_s) exceeded the ACI 318-14 limit of $8\sqrt{f'_c}$ (in psi units; $0.67\sqrt{f'_c}$ *in MPa units*). ACI 318-14 limits the transverse hoop spacing (s) in plastic hinge regions to one quarter of the smallest column dimension for confinement, which is equal to 4.5 in. (115 mm) for all specimens. The hoop spacing for CS60 and CS80 exceeded that limit by one inch, while that limit was met in CS100.

Table 1 - Design parameters and structural analysis results

	b (in.)	h (in.)	cc (in.)	f'_c (ksi)	P_o (kips)	V_e (kips)	M_p (k-in)	a/d	$V_e/\sqrt{f'_c}\,bd$ (psi)
CS60	18	18	1.5	3.83	370	174	7300	2.7	10.1
CS80	18	18	1.5	4.18	370	165	6900	2.7	9.1
CS100	18	18	1.5	4.65	370	168	7070	2.7	8.8
CH100	18	18	1.0	5.21	252	76	4080	3.4	3.6
CL100	18	18	1.0	5.16	252	78	4220	3.4	3.7

b = width of cross section
h = height of cross section in direction of loading
cc = clear cover
f'_c = measured concrete compressive strength at day of testing, mean of three cylinder tests
P_o = applied compressive axial load
V_e = estimated peak shear demands associated with peak moment capacity, M_p
M_p = estimated peak moment capacity evaluated using fiber-section analysis and measured material properties including strain hardening of reinforcing bars
a/d = shear span to cross-section depth ratio
$V_e/\sqrt{f'_c}\,bd$ = estimated peak shear stress demand

Table 2 – Reinforcement details

	Longitudinal Reinforcement						Transverse Reinforcement					
	Bar #	ρ_l	f_y (ksi)	f_t (ksi)	T/Y	$\varepsilon_f (\%)$	Bar #	s (in.)	s / d_b	f_y (ksi)	f_t (ksi)	$\varepsilon_f (\%)$
CS60	10	4.7%	67	95	1.41	18.3	5	5.5	4.4	69	96	14.4
CS80	9	3.7%	79	107	1.34	15.5	4	5.5	4.9	84	111	12.1
CS100	8	2.9%	102	129	1.26	11.6	3	4.5	4.5	119	141	10.1
CH100	6	1.1%	100	127	1.27	11.5	4	3.5	4.7	101	123	12.8
CL100	6	1.1%	106	123	1.16	12.8	4	3.5	4.7	85	100	11.5

ρ_l = ratio of the area of distributed longitudinal reinforcement to gross concrete area perpendicular to that reinforcement
f_y = mean measured yield strengths from three reinforcing bars tested in tension
f_t = mean measured tensile strengths from three reinforcing bars tested in tension
ε_f = mean measured fracture elongations from three reinforcing bars tested in tension
s = spacing of hoops from center-to-center
d_b = bar diameter

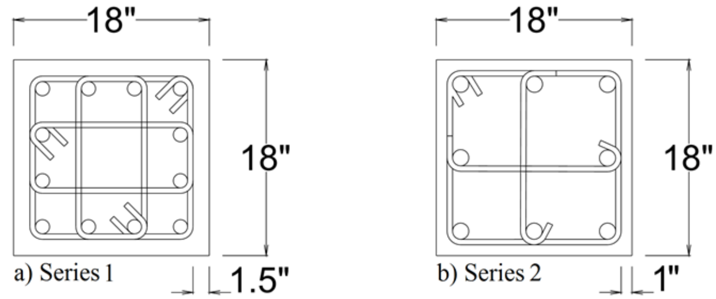

Figure 1 – Cross sectional view of the specimens: a) Series 1 and b) Series 2 (1 in. = 25.4 mm)

Series 2 columns, CH100 and CL100, were reinforced with Grade 100 steel and designed to have similar flexural capacity and associated shear demands. The only difference between the two columns was the steel manufacturing process, which led to differing bar mechanical properties with the T/Y ratio being the main variable (Table 2). Bars from Manufacturer 1 and produced using micro alloying were used in CH100. Bars from Manufacturer 2 achieves higher strength steel by quenching and tempering and were used in CL100. The steel bars used in this series of tests represent the high end of achievable tensile to yield ratio for each production method. Series 2 columns were designed to be 2/3 scale models of prototype columns. As such, the selected clear cover was 1 in. (25.4 mm). Series 2 column columns had a clear height of 108 in. (2740 mm) (Table 1; Table 2; Fig.1). Both columns had 8 #6 longitudinal bars distributed evenly along all four faces (Fig. 1), which resulted in the columns having a similar expected plastic moment strength of 4420 kip-in (500 kN-m), and a corresponding peak shear demand of 83 kips (370 kN) (Table 2). The expected peak shear stress was estimated at $3.6\sqrt{f'_c}$ (in psi units; $0.3\sqrt{f'_c}$ *in MPa units*). Series 2 columns were designed to maximize tension strain demands on the longitudinal bars. Shear stresses were intentionally kept low in the columns to limit the potential beneficial effects of inclined cracking on strain concentrations in longitudinal bars due to tension shift [8]. The axial load applied on these members was 252 kips (1120 kN) corresponding to 15% of the gross capacity of the section. A relatively low level of axial load was chosen in this series so that tension strains in longitudinal bars are not compressed. The transverse reinforcement at each level consisted of a #4 hoop and two #4 cross-ties. Transverse reinforcement spacing was 3.5 in. (90 mm), or 4.7 d_b, for both specimens. This spacing is lower than the 6 d_b spacing required by ACI 318 -14 [1] for Special Moment Frames and closer to the 5 d_b spacing recommended in a report by NIST [9].

2.2 Reinforcing Steel Properties

Reinforcing steel coupons were taken from the same heat as the steel used in each specimen. Three steel samples corresponding to the reinforcing bars in each specimen were tested monotonically in tension to fracture as per ASTM A370 [10]. Table 2 summarizes the three-coupon mean material properties for each specimen. Figure 2 presents typical stress-strain relations for the bars used in the columns. All steel stress-strain curves had a similar shape, with nearly linear behavior up to yielding (f_y) and a well-defined yield plateau. The tensile-to-yield strength ratios (T/Y) gradually decreased as the yield strength increased and ranged from 1.41 for #10 Grade 60 bars to 1.16 for #6 Grade 100 bars in CL100 (Table 2). Likewise, the fracture elongations (ε_f) decreased with increasing yield strength. The higher grade bars did however achieve relatively high fracture elongations which were over 10%.

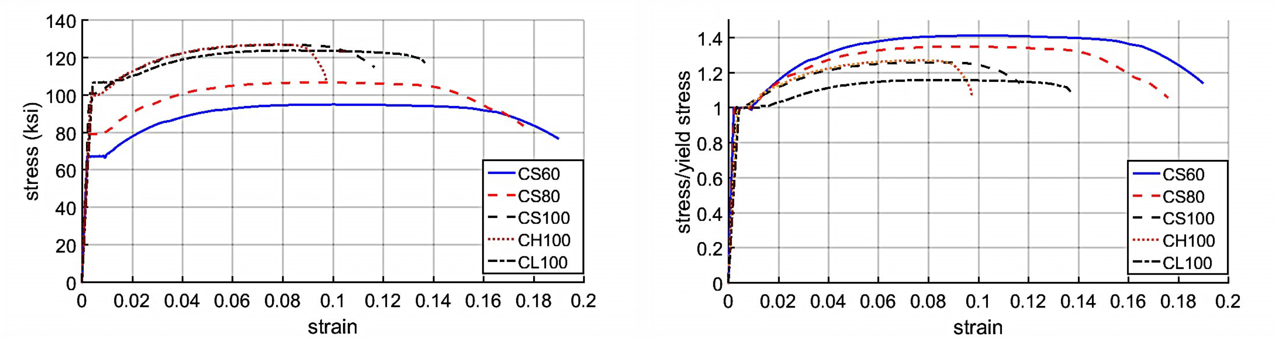

Figure 2 - a) Sample stress-strain plots for longitudinal bars; b) Normalized stress-strain plots for same bars

2.3 Testing and Instrumentation

The specimens were tested under symmetric double curvature with fixed rotation boundary conditions at the top and bottom (Fig. 3). At the beginning of each test, the steel test frame was leveled such that its weight was fully carried by the vertical actuators. Strain and deformations were zeroed at that stage. In all tests, positive drift values imply movement of the columns to the right (or the South direction). In subsequent discussions, drift ratio refers to the lateral drift of a column divided by the column clear height. The I-shaped specimens were fixed to the strong floor at the bottom and steel reaction frame at the top. The axial load was applied by two vertical actuators (Fig. 3). The load was kept constant during the tests. The lateral loading protocol imposed on the specimens consisted of two fully reversed lateral drift cycles at increasing target drifts, following the recommendations of FEMA 461 [11]. The targeted lateral drift ratios were: 0.2%, 0.3%, 0.4%, 0.6%, 0.8%, 1.0%, 1.5%, 2.0%, 3.0%, 4.0%, 5.5%, and 7.0%. Tests were carried in displacement control under slow loading rates.

Figure 3 - Column CS100 and the DIC system during testing

Columns were instrumented to measure the applied loads, distributed surface deformations, and reinforcing bars strains. A Digital Image Correlation (DIC) system developed by the authors was used to measure column surface deformations, from which surface strains and crack widths were obtained [12]. The DIC system tracks targets attached to the surface of the members prior to testing. This system was able to resolve column deformations on the order of 1/10,000th of an inch over the field of view. Targets were placed in a regular 2.75 x 2.75 in. (70 mm x 70 mm) grid over the surface of columns. Strain gauges were installed at points of interest, particularly on the corner bars at the top and bottom interface with the footings where maximum strain demands were expected.

3. Test Results and Discussion

In this section the general behavior of each specimen is presented. Then results regarding strain demands and plasticity spread in longitudinal reinforcement are presented. The general behavior is described through milestones. The first yield of longitudinal reinforcement was identified by following the strain measurements from strain gages on the corner bars. First yield for transverse reinforcement was identified using the DIC system. Previous work by the authors [12] has proven that data gathered from the high resolution DIC system can be used to project the strain in hoops from strains measured on the concrete surface. First inclined and flexural crack was also identified from data gathered with the DIC system. A jump in horizontal or vertical measured strains was used to identify the first inclined or flexural crack, respectively. Peak lateral load represents the maximum load measured during the test. Initiation of lateral strength loss was taken at the point of sudden drop in lateral load resistance of the specimen. Finally, the initiation of axial failure is the first point at which the specimen showed signs of loss of axial strength. This point was accompanied with a shortening of the specimen as indicated by the data gathered from the DIC system [12].

3.1 General Behavior

Series 1 columns CS60 and CS80 showed comparable response up to initiation of lateral-strength loss, which occurred beyond the second excursion to a drift ratio of +5.5%. Initiation of lateral strength loss in CS60 was observed at a drift ratio of +5.2% as the column was being pushed to the first excursion to a drift ratio of +7.0% (Figure 4). The initiation of lateral-strength loss in CS80 occurred at a drift ratio of -4.6% as the column was being pushed to the first excursion to a drift ratio of -7.0% (Figure 4). For both columns, axial collapse occurred right after the initiation of lateral strength loss. As the shear-damaged area contributed to loss of lateral strength, the section could no longer sustain the imposed axial load and vertical sliding occurred across the critical inclined cracks. Column CS60 started losing axial capacity at a drift ratio of +5.8% while CS80 initiated axial failure at a drift ratio of -5.5%. Beyond the initiation of axial failure, column axial loads were reduced gradually to 280 kips (1254 kN) for CS60 and 230 kips (1023 kN) for CS80 as they were pushed monotonically to a drift ratio of +9.1% for CS60 and -8.2% for CS80. No buckling was observed in the longitudinal reinforcement up to the initiation of axial failure. No bar fracture was observed in either CS60 or CS80 at the end of the tests. In conclusion, the Grade 80 (540 MPa) reinforcement preserved the integrity of the concrete core and shear transfer mechanisms to the same high demand levels as the conventional Grade 60 (420 MPa) reinforcement.

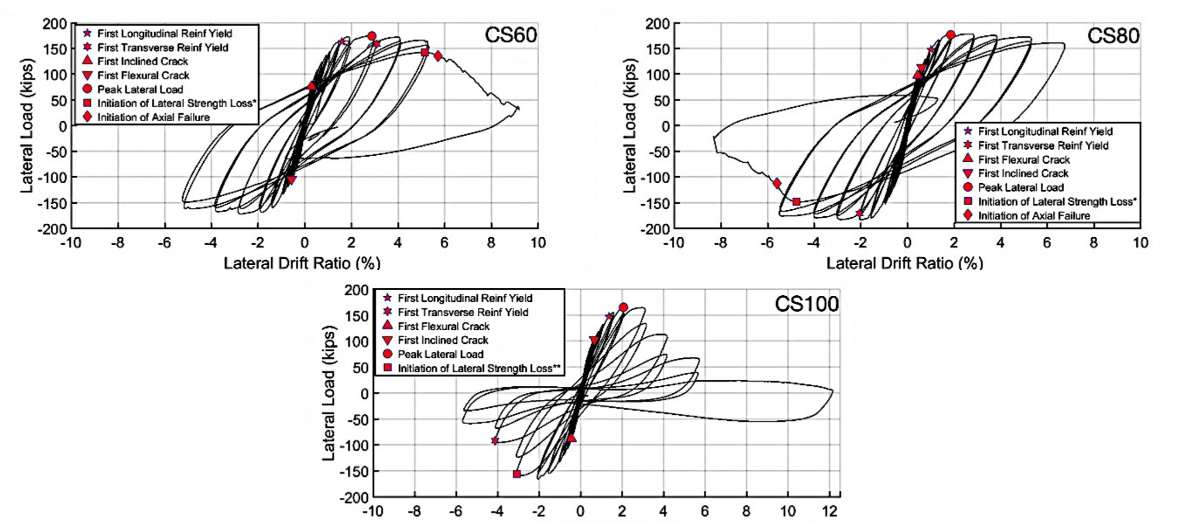

Figure 4 - Lateral load vs. displacement hysteresis for specimens CS60, CS80, and CS100 (1 kip = 4.45 kN)

Similar behavior was observed in column CS100 as in columns CS60 and CS80, up to a drift ratio of 1.5% (Figure 4). The crack pattern in CS100 was similar to those of the other two columns until the end of the 1.5% drift cycles. An increase in the horizontal (x-direction) strains along the outmost longitudinal bars at column ends was measured through the DIC system during the first cycle to a drift ratio of -2.0%. These strains corresponded to longitudinal hairline cracks that formed in the plastic hinge regions at the location of the outer longitudinal bars. As the column was pushed further to the first cycle at a drift ratio of -3.0%, severe longitudinal cracks spread over the height of the column and initiated the lateral strength loss in the column. These bond-splitting cracks caused bond degradation between the longitudinal bars and the concrete. The column was cycled further until significant loss of lateral strength (down to 32 kips (142 kN) or 18.9% of peak strength). The column was pushed monotonically to a drift ratio of +12% drift without loss of axial strength (Figure 3). The bond splitting failure released longitudinal bar stresses as well as the imposed shear forces on the column, which prevented the concrete core from sustaining the shear/axial failure mode observed in the other two columns. Results from this test raised concerns about the minimum allowable length for concrete members reinforced with high strength steel.

It is noted that the bond failure in CS100 only occurred after the concrete surrounding the longitudinal bars degraded sufficiently in the end plastic hinge regions, between drift ratios of 1.5% and 3.0%. This degradation shortened the effective anchorage length of the bars. A recommendation was proposed by Sokoli and Ghannoum [7] to reduce the effective anchorage length of longitudinal bars by 2/3*d* within the plastic hinge regions to account for this loss during inelastic deformations; with *d* = the effective depth of the section from extreme compression fiber ot the centroid of the outermost layer of reinforcing bars. This recommendation was adopted by ACI committee 369 and ASCE committee 41 and will be available in their next standard editions [13].

Series 2 columns CH100 and CL100 reached most major behavioral milestones at almost identical drift levels, as both members had the same design and detailing. Since the design aimed to maximize the strain demands in the longitudinal reinforcement, the first yield occurred relatively early in the loading protocol for both specimens at the end of the first cycle towards a drift ratio of -0.8% (Figure 6). As targeted in the design stage, the specimens showed minor diagonal cracking with most cracks being flexural cracks. Transverse reinforcement in both specimens did not yield. Column CH100 sustained bar fracture at a drift ratio of -3.2% as it was being pushed to the second cycle of -5.5% drift ratio. CL100 completed the 5.5% drift cycles and bar fracture happened at a drift ratio of 4.8% as the column was being pushed to the first cycle of 7.0%. Both specimens maintained the prescribed axial load throughout the tests.

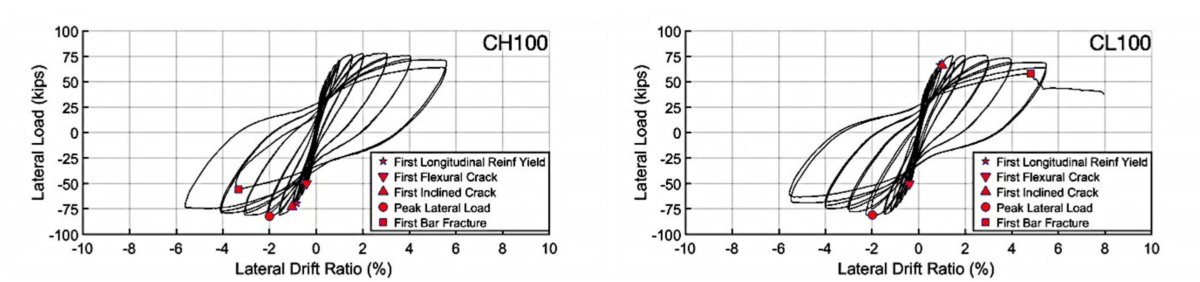

Figure 5 – Lateral load vs. displacement hysteresis for all specimens (1 kip = 4.45 kN)

The envelope of lateral-load versus drift response was very similar for both columns of Series 2, as was the hysteretic behavior. However, CL100 specimen showed up to 10% softer response (measured as the slope of the line connecting the origin to the point of maximum lateral load of each cycle) when compared to the same cycle of CH100. Because of the relatively low amount of damage through the cycles, the softening also remained relatively small from cycle to cycle, until the longitudinal reinforcement buckled. After buckling of longitudinal reinforcement the responses degraded significantly from cycle to cycle. Mechanical properties of the reinforcement did not dictate major differences between the overall behaviors of the two specimens.

In conclusion, although there are no set targets for satisfactory behavior, a stable response up to a drift ratio of 4% is generally considered to be a minimum performance objective for collapse prevention at the Maximum Considered Earthquake (MCE) hazard level. Specimens CS60, CS80, CH100, and CL100, all remained stable at least up to a drift ratio of 5.5%. Shear stresses and associated bond demands on the order of $10\sqrt{f'_c}$ (in psi units, *$0.83\sqrt{f'_c}$ in MPa units*) proved to be excessive for the column reinforced with Grade 100 steel. A limit in the form of shear stresses or member minimum length should be set in order to avoid bond failures.

3.2 Strain Demands

The largest longitudinal-bar tensile strains in Series 1 columns are plotted at each drift target for each column in Figure 6. The #10 (d_b = 1.25" (32 mm)) Grade 60 (420 MPa) bars used as longitudinal reinforcement in CS60 had an average yield strain of 0.0023 as measured from coupon tests, which was reached at a drift ratio of +1.6%, in the first cycle toward a drift target of 2.0%. The #9 (d_b = 1.13" (29 mm)) Grade 80 (540 MPa) bars had an average measured yield strain of 0.0027. This strain was achieved at the end of the first cycle toward a drift ratio of 1.0%. The longitudinal bars in CS100 reached their average yield strain of 0.0035 at the end of the first cycle toward a drift ratio of 1.0%. As can be seen Figure 6, the Grade 80 (540 MPa) longitudinal bars in CS80 saw significantly larger strains at all drift levels, and were up to 65% higher, than those in longitudinal bars of CS60. The longitudinal bars in CS100 did not reach as high strains as those in the other two columns due to the premature bond-splitting failure. However, longitudinal bars in CS100 had significantly higher strains (about 25% higher than in CS80 and 100% higher than in CS60) up to the end of the 1.5% drift cycles and prior to significant loss of bond. The recorded strain amplitudes in the longitudinal bars of the tested columns were relatively low owing to the relatively high axial load. However, the observed larger strains in the HSRB compared with Grade 60 (420 MPa) bars raises the concern that HSRB may fracture prematurely compared with Grade 60 (420 MPa) counterparts in applications where large strain amplitudes are expected (e.g., concrete columns or walls with low axial loads). This observation motivated the columns tests of Series 2.

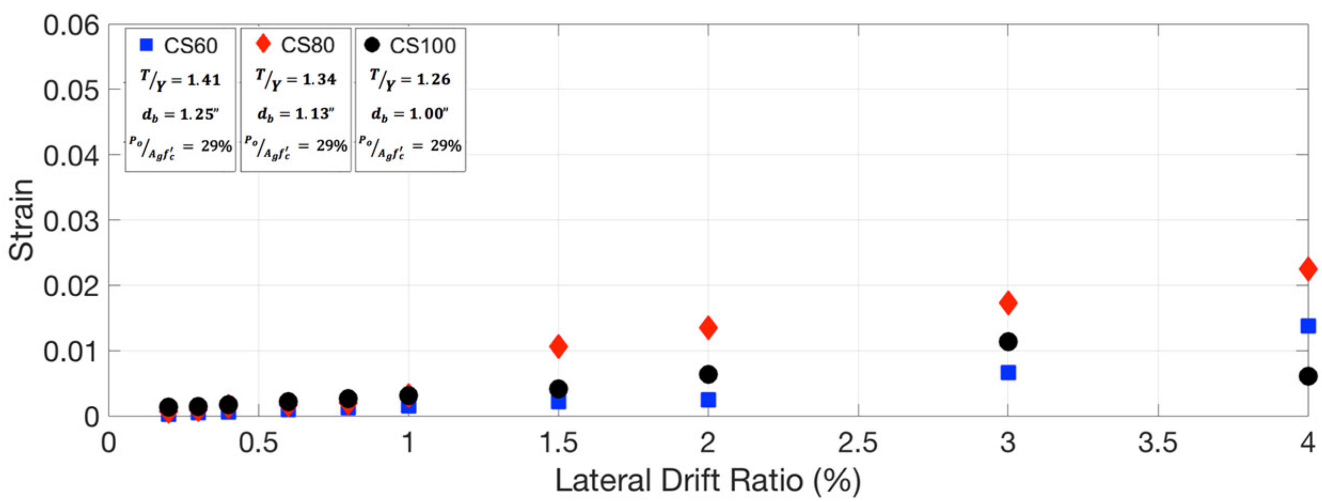

Figure 6 – Series 1 measured tensile strains vs. drift ratio

The maximum longitudinal-bar tensile strains measured in Series 2 columns are plotted in Figure 7 at each drift target. The #6 bars used as longitudinal reinforcement in CH100 had an average yield strain of 0.0033, while the #6 bars in CL100 had an average measured yield strain of 0.0041. Both these columns reached their yield strain at the end of the first cycle toward a drift ratio of -0.8%. As can be seen in Figure 7, the Grade 100 longitudinal bars in CL100 saw significantly larger strains at all drift levels, and were up to 34% higher at a drift ratio of 4.0%, than those in the longitudinal bars of CH100.

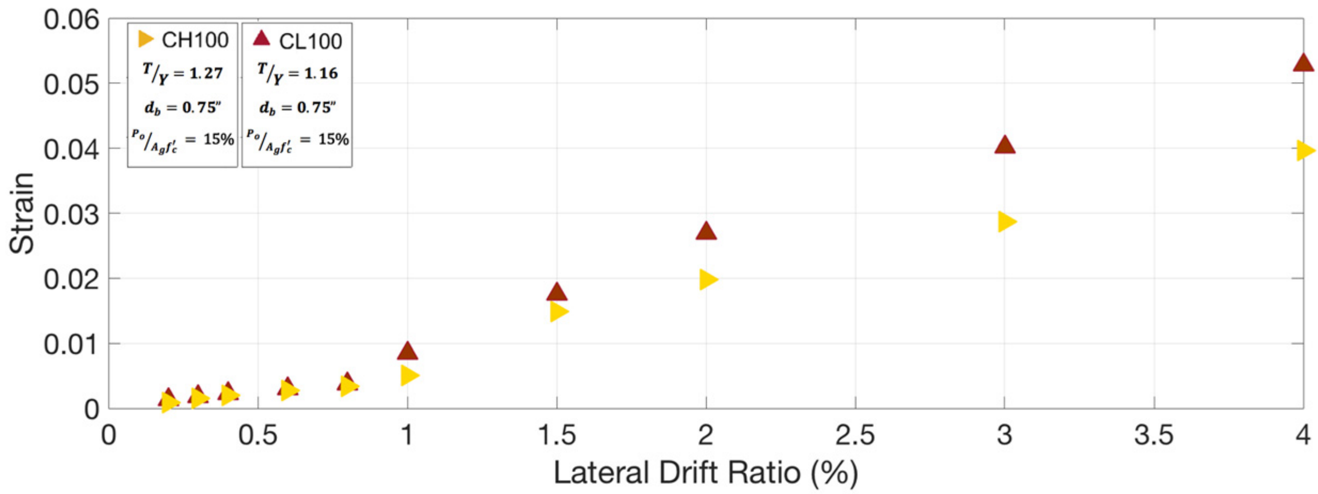

Figure 7 - Second series measured tension strain vs. drift ratio

Figure 8 presents typical measured strains in the longitudinal reinforcement over the height of columns CL100 and CH100 at different drift ratios. This plot further demonstrates that specimen CL100 saw strain concentration at the points of peak demand. Figure 8 further indicates that the higher peak strains at the point of maximum demand in CL100 were associated with reduced strain demands away from the point of peak demands compared with what was recorded in CH100. This tendency of reinforcement with lower T/Y to magnify bar strain demands and limit plasticity spread could lead to premature member failures due to low-cycle fatigue fracture of bars. Slavin and Ghannoum [14] demonstrated that a 100% increase in strain amplitudes can lead to an order of magnitude reduction in the number of cycle to fracture of reinforcing bars. Yet, column CL100 was pushed to similar drift targets as CH100 without prior to any bar fracturing. This could be due to the higher fracture elongation, ε_f, of the reinforcement in CL100. Alternatively, the bars with the lower T/Y ratio may have had longer fatigue life than those with the higher T/Y ratio.

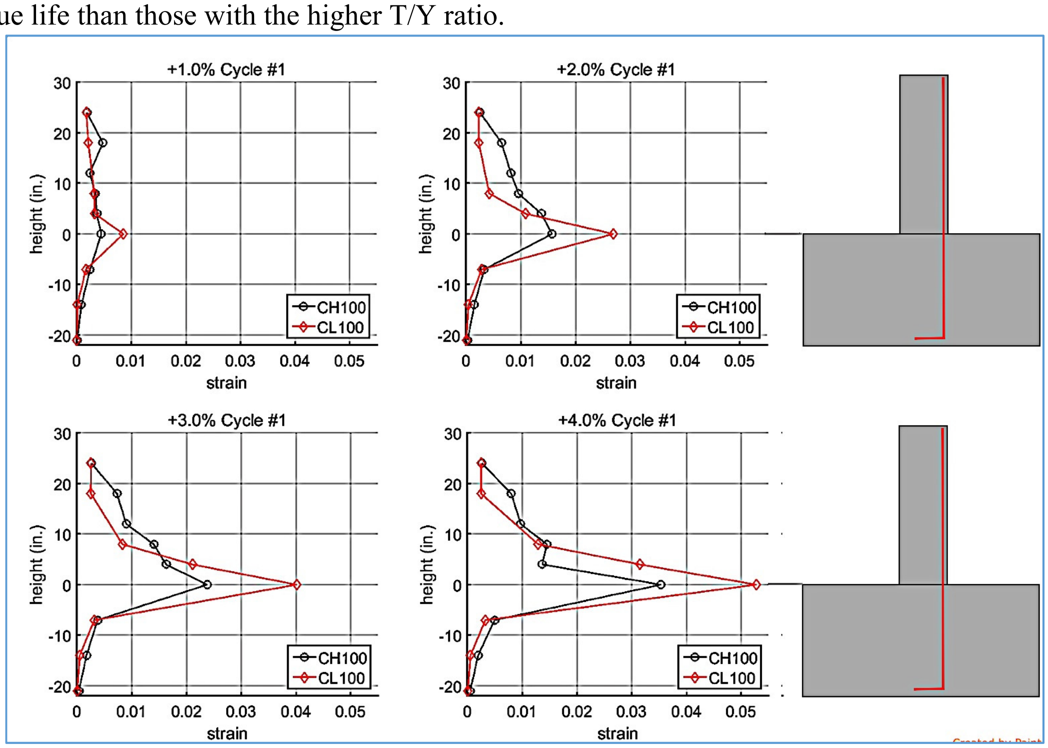

Figure 8 – Sample measured strain profiles over column height (1 in. = 25.4 mm)

4. Conclusions

Columns CS60, CS80, CH100, and CL100, exhibited stable cyclic responses up to a drift ratio of 5.5%, which can be considered satisfactory for collapse prevention at the Maximum Considered Earthquake (MCE) hazard level. Test results therefore indicate that higher grade reinforcing bars, up to Grade 100 (100 ksi specified yield strength (690 MPa)) may be suitable for use in both longitudinal and transverse reinforcement in regions of high seismicity.

Column CS100 sustained a bond failure around the longitudinal bars, which raised concerns about the minimum allowable length for concrete members reinforced with high strength steel. Shear stresses on the order of $10\sqrt{f'_c}$ (psi units) proved to be excessive for that member, which was reinforced with Grade 100 (690 MPa) steel. A limit in the form of shear stresses or member minimum length is advised for higher strength bars to avoid bond failures. Accounting for the loss of bond strength within plastic hinge regions is also advised for all bar grades.

Higher strain demands were observed in higher strength longitudinal bars. This trend was attributed in part to differences in the tensile-to-yield strength (*T/Y*) ratios of various bars used in the experimental program. As is typical in reinforcing bar production, the *T/Y* ratio of the bars used in this study dropped as the bar strength increased. In the first series, the measured *T/Y* ratio for the longitudinal reinforcement reduced from 1.41 in CS60 to 1.26 in CS100. The effect of the T/Y ratio on plasticity spread was isolated in the Series 2 tests, in which the only variable was the T/Y ratio of the Grade 100 bars, and in which longitudinal bars with the lower T/Y ratio experienced larger strain demands at any given column drift demand. Lower *T/Y* ratios reduce the ability of bars to spread their inelastic strains away from flexural crack locations, which results in amplified peak strain demands. The higher strain demands on higher-strength bars in turn raised concerns about their low-cycle fatigue behavior and possible premature fractures in application with high strain-cycle demands.

5. Acknowledgements

The experimental program was conducted through generous financial support from the Charles Pankow Foundation, the Concrete Reinforcing Steel Institute, the American Concrete Institute’s Foundation, and NUCOR Steel Inc. Seattle. Donations of reinforcing bars and their fabrication by CMC and NUCOR Steel Inc. Seattle are gratefully acknowledged, as is the technical guidance provided by Mike Mota of CRSI, Erik Nissen of NUCOR Steel, and Jacob Seltzer of CMC regarding reinforcing bar manufacturing and metallurgy.

5. References

[1] ACI Committee 318, (2014). “Building Code Requirements for Structural Concrete (ACI 318-14) and Commentary (ACI 318R-14),” American Concrete Institute, Farmington Hills, MI, 519 pp.

[2] Aoyama, H. (2001). "Design of Modern Highrise Reinforced Concrete Structures.“ Imperial College Press, London, UK.

[3] Macchi, G., Pinto, P. E., and Sanpaolesi, L. (1996). "Ductility requirements for reinforcement under Eurocodes“ Structural Engineering International, **6**(4), 249-254.

[4] ATC-115, (2015). “Roadmap for the Use of High-Strength Reinforcement in Reinforced Concrete Design,” Applied Technology Council, 197 pp.

[5] Sokoli, D., (2014). “Seismic Performance of Concrete Columns Reinforced with High Strength Steel,” master’s thesis, University of Texas at Austin, Austin, TX, 166 pp.

[6] Sokoli, D., and Ghannoum, W. M., (2016). “High-Strength Reinforcement in Columns under High Shear Stresses,” ACI Structural Journal, V. 113, No. 3, pp. 605-614.

[7] ASTM Standard A706/A706M-13, (2013). “Standard Specification for Low-Alloy Steel Deformed and Plain Bars for Concrete Reinforcement.” ASTM International, West Conshohocken, PA.

[8] Paulay, T. and M.J.N. Priestley, (1992). “Seismic Design of Reinforced Concrete and Masonry Buildings. John Wiley and Sons, Inc. 744.

[9] NEHRP Consultants Joint Venture (2014). "Use of High-Strength Reinforcement in Earthquake-Resistant Concrete Structures," Washington DC p. 231.

[10] ASTM A370-14, (2014). "Standard Test Methods and Definitions for Mechanical Testing of Steel Products," ASTM International, West Consho- hocken, PA, 2014, 50 pp.

[11] FEMA, "Interim Testing Protocols for Determining the Seismic Performance Characteristics of Structural and Nonstructural Components (FEMA- 461)," Federal Emergency Management Agency, Washington, DC, 2007, 138 pp.

[12] Sokoli, D.; Shekarchi, W.; Buenrostro, E.; and Ghannoum, W. M., (2014). "Advancing Behavioral Understanding and Damage Evaluation of Concrete Members Using High-Resolution Digital Image Correlation Data," Earthquakes and Structures, V. 7, No. 5, pp. 609-626. doi: 10.12989/eas.2014.7.5.609

[13] Ghannoum, W.M., Updates To Modeling Parameters And Acceptance Criteria For Non-Ductile And Splice-Deficient Concrete Columns, 16 WCEE, Paper 1010, Santiago Chile, January 2017

[14] Slavin, C.M. and W.M. Ghannoum, (2015). "Defining Structurally Acceptable Properties of High-Strength Steel Bars through Material and Column Testing," PART I: MATERIAL TESTING REPORT, Charles Pankow Foundation, p. 135.